Journal of Alloys and Compounds, 189 (1992) 221–228
JALCOM 379

Er_2RhSi_3 and R_2CoGa_3 (R ≡ Y, Tb, Dy, Ho, Er, Tm, Yb) with Lu_2CoGa_3 type structure: new members of the AlB_2 structure family

R. E. Gladyshevskii, K. Cenzual and E. Parthé
Laboratoire de Cristallographie, Université de Genève, 24 quai Ernest-Ansermet, CH-1211 Geneva 4 (Switzerland)

(Received May 29, 1992)

Abstract

The structure of Er_2RhSi_3 was redetermined by X-ray single-crystal diffraction (λ(Mo Kα) = 0.71073 Å, μ = 42.392 mm^{-1}, $F(000) = 892$, $T = 293$ K, $R = 0.037$, $wR = 0.030$ for 244 contributing unique reflections). It is shown that this silicide has a hexagonal structure of the Lu_2CoGa_3 type, *hP*24, (194) $P6_3/mmc$-*khfb*, $a = 8.1130(7)$, $c = 7.7556(9)$ Å, $V = 442.09(9)$ Å^3, $Z = 4$, $M_r = 521.68$, $D_x = 7.838$ mg mm^{-3}. The structure of isotypic $Er_2Co_{1.4}Ga_{2.6}$ (*hP*24, (194) $P6_3/mmc$-*khfb*, $a = 8.607(3)$, $c = 6.898(3)$ Å, $V = 442.5(4)$ Å^3, $Z = 4$, $M_r = 598.30$, $D_x = 8.980$ mg mm^{-3}) was refined by X-ray powder diffraction (λ(Fe Kα) = 1.93735 Å, $F(000) = 1017.6$, $T = 293$ K, $R = 0.092$ for 61 reflections). The cell parameters of $R_2Co_{1+x}Ga_{3-x}$ phases (R ≡ Y, Tb, Dy, Ho, Er, Tm, Yb; $x = \pm 0.4$) with the same structure type were obtained from X-ray powder diagrams. The Lu_2CoGa_3 structure is a distorted substitution variant of the AlB_2 type, where the trigonal Lu_6 prisms centred by cobalt atoms share triangular faces in infinite columns. The cobalt atoms are displaced away from the prism centres like the mercury atoms in the orthorhombic KHg_2 structure type. The distortions in Er_2RhSi_3 are of a lesser magnitude than those observed in Lu_2CoGa_3. A progressive substitution of gallium by cobalt along the RGa_2–RCoGa cross-sections of the R–Co–Ga systems (R ≡ Y, Tb, Dy, Ho, Er, Tm, Yb, Lu) leads to a step by step deformation of the trigonal prisms. The main features of other deformation and substitution derivatives of the AlB_2 type are discussed.

1. Introduction

A series of rare-earth metal–rhodium silicides was reported by Chevalier *et al.* to crystallize with a new, AlB_2-related structure type [1]. The structure of Er_2RhSi_3 was refined from X-ray powder spectra and the authors state that the best agreement between calculated and observed line intensities was obtained for the space group $P\bar{6}2c$. However, a study of the atomic coordinates shows that the deviations from centrosymmetricity are very small indeed.

During systematic investigations of rare-earth metal–cobalt–gallium systems [2], the new compound Lu_2CoGa_3 was identified [3]. It crystallizes in the space group $P6_3/mmc$ with a structure which is very similar to that reported for Er_2RhSi_3. We report here on the redetermination of the structure of Er_2RhSi_3, motivated by its possible isotypism with Lu_2CoGa_3. It also seemed of interest to extend the analysis to other members of the AlB_2 structure family and to study the effect of progressive cobalt substitution in some rare-earth metal digallides.

2. Experimental details

A sample of nominal composition Er_2RhSi_3 was prepared from high purity elements (erbium and rhodium 99.9%, silicon 99.999%) by arc melting under an argon atmosphere (the mass loss was 0.6%), annealing at 1073 K for two weeks in a silica tube under an argon atmosphere (5.3×10^4 Pa) and quenching in water. A single crystal (dimensions, ±(100) 0.054 mm, ±(010) 0.052 mm, ±(001) 0.026 mm) was mounted on a Philips PW1100 automatic four-circle diffractometer (Mo Kα radiation, graphite monochromator). The unit-cell parameters refined from 2θ values of 21 reflections (Mo Kα, $\lambda = 0.71073$ Å, $15° < 2\theta < 35°$) are in good agreement with those reported in ref. 1. 1042 reflections were collected out to $\sin\theta/\lambda = 0.702$ Å^{-1} ($0 \leqslant h \leqslant 9$, $0 \leqslant k \leqslant 9$, $0 \leqslant l \leqslant 10$ and their antireflections) in the ω–2θ scan mode, yielding 275 unique reflections ($R_{int} = 0.036$). Two standard reflections, 202 and 220, showed a maximum intensity variation of 1.2%. An absorption correction was made using the program LSABS, described in ref. 4, with minimum and maximum transmission factors of 0.0757 and 0.1515. The anomalous dispersion coefficients were taken from ref. 5. Systematic absences led to the following possible space groups: $P6_3mc$, $P\bar{6}2c$ and $P6_3/mmc$ [6]. The isotypism with Lu_2CoGa_3 was confirmed by the structure refinement, based on $|F|$ values. 17 variables, including anisotropic atomic displacement parameters, were refined to $R = 0.037$ and

0925-8388/92/$5.00

TABLE 1. Structure data for Er_2RhSi_3, $Er_2Co_{1.4}Ga_{2.6}$ and Lu_2CoGa_3 (*hP*24, (194) $P6_3/mmc$-*khfb*, $Z=4$)

Atom	Wyckoff position	*x*	*y*	*z*	$U_{eq}\times10^2$ (Å^2)
Er_2RhSi_3: $a=8.1130(7)$, $c=7.7556(9)$ Å, $V=442.09(9)$ Å^3					
Si	12(*k*)	0.1669(2)	2*x*	0.0014(4)	0.78(9)
Er(1)	6(*h*)	0.50914(5)	2*x*	1/4	0.75(3)
Rh	4(*f*)	1/3	2/3	0.0324(2)	0.69(4)
Er(2)	2(*b*)	0	0	1/4	0.65(3)
$Er_2Co_{1.4}Ga_{2.6}$: $a=8.607(3)$, $c=6.898(3)$ Å, $V=442.5(4)$ Å^3					
$Ga_{0.87(7)}Co_{0.13(7)}$	12(*k*)	0.158(3)	2*x*	0.043(6)	1.4(9)
Er(1)	6(*h*)	0.523(1)	2*x*	1/4	2.0(5)
Co	4(*f*)	1/3	2/3	0.065(6)	1.3(8)
Er(2)	2(*b*)	0	0	1/4	2.2(6)
Lu_2CoGa_3[a]: $a=8.659(2)$, $c=6.823(1)$ Å, $V=443.0(2)$ Å^3					
Ga	12(*k*)	0.1692(2)	2*x*	0.0432(2)	1.41(9)
Lu(1)	6(*h*)	0.5231(1)	2*x*	1/4	1.05(4)
Co	4(*f*)	1/3	2/3	0.050(1)	1.6(1)
Lu(2)	2(*b*)	0	0	1/4	0.87(6)

The equivalent isotropic atomic displacement parameters are expressed as $U_{eq}=(1/3)\Sigma_i\Sigma_j U_{ij}a_i^*a_j^*a_i\cdot a_j$; for $Er_2Co_{1.4}Ga_{2.6}$ isotropic displacement parameters were refined.
[a]From ref. 3.

TABLE 2. Interatomic distances (in ångströms) in Er_2RhSi_3, $Er_2Co_{1.4}Ga_{2.6}$ and Lu_2CoGa_3

Er_2RhSi_3		$Er_2Co_{1.4}Ga_{2.6}$		Lu_2CoGa_3	
Er(1)–2Rh	2.992	Er(1)–2Co	3.05	Lu(1)–2Co	2.971
4Si	2.999	4Ga*	3.08	4Ga	3.024
4Si	3.084	2Co	3.10	4Ga	3.066
2Rh	3.114	4Ga*	3.15	2Co	3.156
2Er(1)	3.834	2Er(1)	3.52	2Lu(1)	3.481
2Er(1)	3.886	2Er(1)	3.71	2Lu(1)	3.729
2Er(2)	4.058	2Er(2)	4.32	2Lu(2)	4.343
2Er(1)	4.279	2Er(1)	4.90	2Lu(1)	4.930
Er(2)–6Si	3.036	Er(2)–6Ga*	2.75	Lu(2)–6Ga	2.904
6Si	3.050	6Ga*	3.10	6Ga	3.231
2Er(2)	3.878	2Er(2)	3.45	2Lu(2)	3.412
6Er(1)	4.058	6Er(1)	4.32	6Lu(1)	4.343
Rh–3Si	2.351	Co–Co	2.55	Co–3Ga	2.462
3Er(1)	2.992	3Ga*	2.62	Co	2.729
3Er(1)	3.114	3Er(1)	3.05	3Lu(1)	2.971
Rh	3.375	3Er(1)	3.10	3Lu(1)	3.156
Si–2Si	2.345	Ga*–2Ga*	2.43	Ga–Co	2.462
Rh	2.351	Co	2.62	2Ga	2.605
2Er(1)	2.999	Er(2)	2.75	Ga	2.822
Er(2)	3.036	Ga*	2.86	Lu(2)	2.904
Er(2)	3.050	2Er(1)	3.08	2Lu(1)	3.024
2Er(1)	3.084	Er(2)	3.10	2Lu(1)	3.066
Si	3.856	2Er(1)	3.15	Lu(2)	3.231

Ga* is $Ga_{0.87}Co_{0.13}$. E.s.d.s are less than 0.005, 0.07 and 0.010 Å for Er_2RhSi_3, $Er_2Co_{1.4}Ga_{2.6}$ and Lu_2CoGa_3 respectively.

$wR=0.030$ ($w=1/\sigma^2(|F_{rel}|)$, $S=2.647$), considering 244 contributing reflections with $|F_{rel}|>3\sigma(|F_{rel}|)$. A secondary-extinction correction parameter (Gaussian distribution of mosaic spread) was refined to $G=0.0054(4)$. The maximum shift per e.s.d. in the last cycle was 0.2×10^{-4} and the final residual electron density $+7.6(-7.1)$ electrons Å^{-3}.* The programs used to

*Further details of the structure determination (*e.g.* structure factors) can be ordered from the Fachinformationszentrum Karlsruhe, D-7514 Eggenstein-Leopoldshafen (deposition No 300248).

TABLE 3. Unit-cell parameters for $R_2Co_{1+x}Ga_{3-x}$ phases ($x = \pm 0.4$) with Lu_2CoGa_3 structure type

R	$a \pm 0.003$ (Å)		$c \pm 0.003$ (Å)		$V \pm 0.4$ (Å^3)	
	$x = -0.4$	$x = +0.4$	$x = -0.4$	$x = +0.4$	$x = -0.4$	$x = +0.4$
Y	8.727	8.660	7.169	7.014	472.8	455.5
Tb	8.764	8.680	7.095	7.037	471.9	459.2
Dy	8.740	8.653	7.048	6.994	466.3	453.5
Ho	8.735	8.630	7.012	6.945	463.3	447.9
Er	8.717	8.607	6.979	6.898	459.3	442.5
Tm	8.704	8.591	6.940	6.853	455.3	438.0
Yb		8.858		7.239		491.9
Lu	8.652	8.560	6.801	6.785	440.9	430.6

refine the structure were all from the XTAL3.0 system [7]. The atomic positional parameters were standardized using the STRUCTURE TIDY program [8]. The final structural data for Er_2RhSi_3 are given in Table 1 and the interatomic distances in Table 2. Attempts to refine the structure in the non-isomorphic subgroup (190) $P\bar{6}2c$, chosen in ref. 1, did not improve the results and we conclude that the structure is centrosymmetric. The compounds with the same stoichiometry found in the {Y, La, Ce, Nd, Sm, Gd, Tb, Dy, Ho}–Rh–Si systems and reported to be isotypic with Er_2RhSi_3 [1] probably also crystallize in space group $P6_3/mmc$.

Rare-earth metal–cobalt–gallium compounds of compositions $R_2Co_{0.6}Ga_{3.4}$ and $R_2Co_{1.4}Ga_{2.6}$ (R ≡ Y, Tb, Dy, Ho, Er, Tm, Yb) were also prepared by arc melting under an argon atmosphere. The samples were annealed at 873 K (ytterbium-containing samples at 673 K) for two weeks in a silica tube under vacuum and quenched in water. They were investigated by powder X-ray diffraction (diffractometer DRON-2.0, Fe Kα radiation, $\lambda = 1.93735$ Å, internal silicon standard $a = 5.4308$ Å) and found to be isotypic with Lu_2CoGa_3. The unit-cell parameters are listed in Table 3. The structure of $Er_2Co_{1.4}Ga_{2.6}$ was refined from 61 reflections ($40° < 2\theta < 108°$) to $R = 0.092$ using programs from the PMNK system [9]. The standardized atomic parameters are given in Table 1 and the interatomic distances in Table 2.

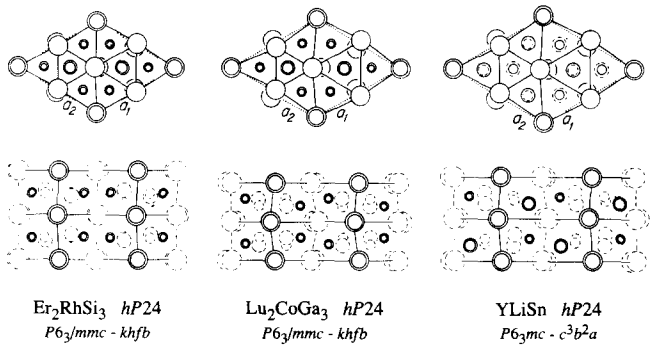

Fig. 1. The structures of Er_2RhSi_3, Lu_2CoGa_3 and YLiSn in projections along [0001] and [11$\bar{2}$0]. Large circles are erbium, lutetium or yttrium; medium circles are rhodium, cobalt or lithium; small circles are silicon, gallium or tin. Double full circles represent atoms of the same element which are superposed in projection in the translation unit.

3. Discussion

3.1. The crystal structures of the title compounds

Projections of Er_2RhSi_3 and Lu_2CoGa_3 along [0001] and [11$\bar{2}$0] are shown in Fig. 1. The Lu_2CoGa_3 type structure is a member of the AlB_2 family with an ordered arrangement of cobalt and gallium atoms inside face-sharing, distorted trigonal Lu_6 prisms. The ordering of the cobalt and gallium atoms is such that the cobalt-centred prisms share triangular faces to form infinite columns. The common faces are alternatively larger and smaller and the cobalt atoms are displaced away from the centres of the prisms, along the 3-fold axes, towards the larger face. In this way, Co–Co dumb-bells appear with an interatomic distance of 2.73 Å. The gallium atoms are arranged in puckered hexagons (distance Ga–Ga 2.60 Å) which are loosely interconnected (distance Ga–Ga 2.82 Å) to form a tubular framework around the c-axis.

Isotypic compounds are found in the R–Co–Ga systems where R ≡ Y, Tb, Dy, Ho, Er, Tm, Yb [2]. Up to 13% of the gallium atoms in these R_2CoGa_3 compounds can be replaced by cobalt atoms. It can be seen from Table 1 that only the site 12(k) in $Er_2Co_{1.4}Ga_{2.6}$ has mixed Ga–Co occupation. On the other side of the ordered stoichiometry, substitution of up to 40% of the cobalt atoms by gallium atoms is possible and one expects to find a mixed occupation of the site 4(f). With increasing cobalt content, which has a smaller atomic radius than gallium, the unit-cell parameters decrease within the homogeneity range (see Table 3). In a similar way, when the atomic number of the rare-earth metal increases (and the atomic radius becomes smaller owing to the lanthanide contraction), the unit-

cell volume decreases. It can be seen from Table 2 that the Co–Co dumb-bells in $Er_2Co_{1.4}Ga_{2.6}$ are even shorter (2.55 Å) than in Lu_2CoGa_3, whereas the 3-fold connexion of the Ga* (*i.e.* $Ga_{0.87}Co_{0.13}$) atoms is less outstanding (distance inside hexagons 2.43 Å, distance between hexagons 2.86 Å) than in the fully ordered Lu_2CoGa_3 compound.

For Er_2RhSi_3 the distortions from the AlB_2-type atom arrangement with regular centred trigonal prisms are smaller than for the gallides. The rhodium atoms are only slightly displaced from the prism centres in such a way that the shortest Rh–Rh distance becomes 3.38 Å. The silicon atoms form isolated, approximately planar hexagons (distance Si–Si inside the hexagons 2.34 Å, shortest distance between hexagons 3.86 Å). An undistorted substitution variant of the AlB_2 type with the same atom ordering would crystallize in the space group *P6/mmm-mfda*, *hP*12, with cell parameters $a' = a$ and $c' = c/2$ compared with Er_2RhSi_3.

An ordered substitution variant of the Lu_2CoGa_3 type, reported for equiatomic YLiSn [10], is also presented in Fig. 1. The deformations are of similar magnitude to those observed for Lu_2CoGa_3 but the homogeneous ordering of the prism-centring lithium and tin atoms lowers the symmetry to space group $P6_3mc$. These atoms form a distorted tetrahedral wurtzite-type framework, without homonuclear contacts.

The partly disordered structure of $CaZn_3$ [11] crystallizes with the same space group as Lu_2CoGa_3 and similar unit-cell parameters. It was described in terms of two types of atom arrangement, statistically distributed in the crystal. One of them is nearly identical with the structure of $BaLi_4$ [12], whereas the second, which was shown to be related to the KHg_2 type structure [13], is in fact a binary variant of the Lu_2CoGa_3 type.

3.2. *Other deformation and substitution derivatives of the AlB_2 type*

Figures 2, 3 and 4 show a series of other structure types belonging to the AlB_2 structure family. Those in Fig. 2 can be derived from the parent type by deformation, whereas Figs. 3 and 4 contain ordered substitution variants which are more or less strongly distorted with respect to the AlB_2 type. Some of the structures correspond to structure type branches which are generally separated in the literature [14, 15], *i.e.* AlB_2 and UHg_2, $EuGe_2$ and $CeCd_2$, NdPtSb and LiGaGe, and HoNiGa, BiSCl and TiNiSi.

In the structure of AlB_2 [16], shown in Fig. 2, aluminium atom layers with triangle mesh (3^6) alternate with boron atom layers with hexagon mesh (6^3). The boron atoms are coordinated by tri-capped trigonal prisms of composition Al_6B_3, whereas the aluminium atoms centre hexagonal B_{12} prisms, all faces of which are capped by aluminium atoms.

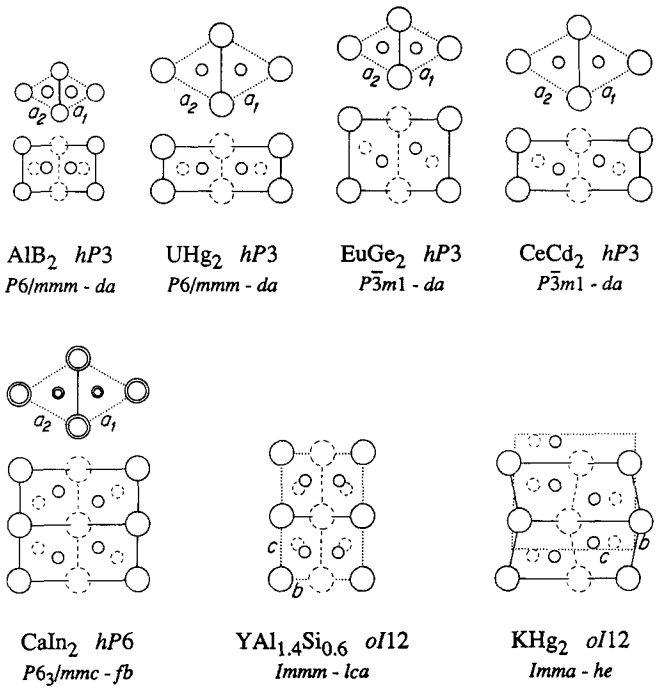

Fig. 2. The structures of AlB_2 and its binary deformation variants. Large circles correspond to the first element in the chemical formula.

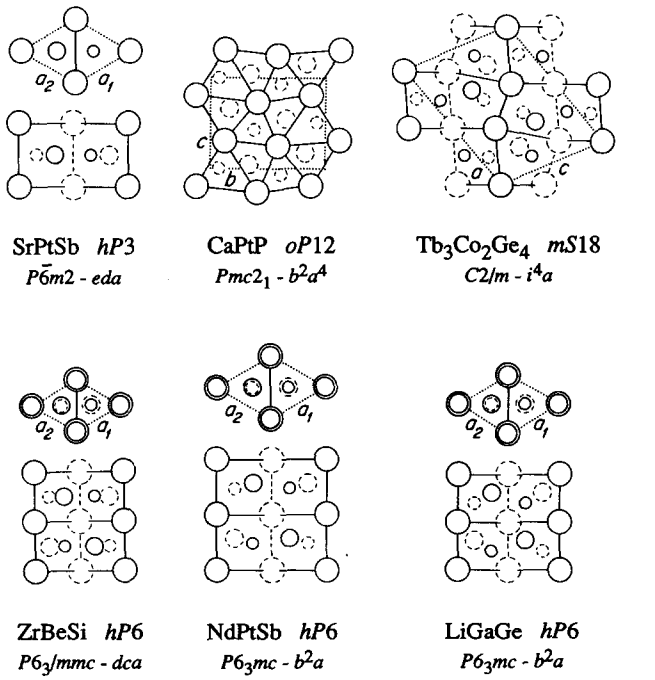

Fig. 3. The structures of ternary substitution derivatives of the AlB_2 type (I). Large circles correspond to the first, medium circles to the second and small circles to the last element in the chemical formula.

Six different binary or pseudo-binary deformation variants of the AlB_2 type are known. For the UHg_2 [17] branch of AlB_2 the c/a ratio is significantly smaller than for AlB_2 itself (0.65 compared with 1.08). The

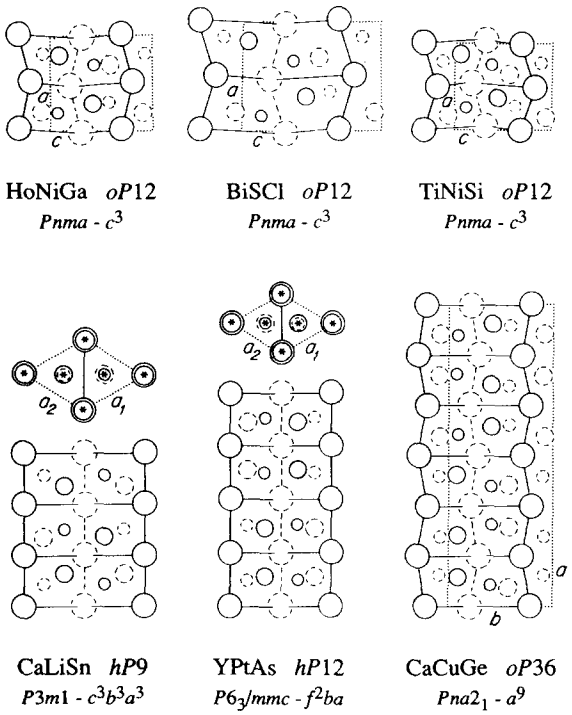

Fig. 4. The structures of ternary substitution derivatives of the AlB_2 type (II). Large circles correspond to the first, medium circles to the second and small circles to the last element in the chemical formula, except for BiSCl where the order is reversed. Asterisks indicate more than two superposed atoms in projection in the translation unit.

mercury atoms situated above and below the triangular faces of the prisms are at a contact distance to the central atom, the coordination number of which consequently increases to 11. In trigonal $CeCd_2$ [18] ($c/a = 0.68$) and its branch $EuGe_2$ [19] ($c/a = 1.22$), the atoms centring the trigonal prisms (cadmium and germanium respectively) are displaced along the prism axis and form puckered hexagon mesh layers. The 3-fold connection of the germanium atoms in $EuGe_2$ is in agreement with the generalized 8-*N* rule for polyanionic valence compounds. In hexagonal $CaIn_2$ [20] similar puckered layers, formed by the indium atoms, are interconnected. Consecutive layers are related by a mirror plane and the *c*-parameter is doubled with respect to the cell of AlB_2. $CaIn_2$ is a Zintl compound where the indium atoms are arranged in a three-dimensional tetrahedral framework. In $YAl_{1.4}Si_{0.6}$ [21] and KHg_2 [13] different distortions of the hexagon mesh layers, leading both structures to show orthorhombic symmetry, are observed. In KHg_2 the trigonal prisms are distorted in such a way that each prism has one smaller and one larger triangular face. The mercury atoms are displaced towards the larger face and form a three-dimensional framework where each atom is surrounded by four others in a distorted tetrahedral coordination.

A number of ordered substitution variants of AlB_2 are known where the trigonal prisms are centred by two kinds of atom in the ratio 1:1. The simplest of these derivatives, which has the same number of atoms in the unit cell as AlB_2, was identified for SrPtSb [22] ($c/a = 1.00$). Two projections of this hexagonal structure, along [0001] and [11$\bar{2}$0], are shown in Fig. 3. Platinum atoms cap the rectangular faces of those trigonal Sr_6 prisms which are centred by antimony atoms and *vice versa*. The strontium atoms centre mixed hexagonal prisms of composition Pt_6Sb_6, capped by eight strontium atoms. In the orthorhombic distorted variant CaPtP [23], the deformations in the planes perpendicular to the prism axes are such that Pt–Pt pairs appear (2.85 Å) and the hexagonal prisms surrounding half of the calcium atoms are transformed to pentagonal prisms.

In SrPtSb and CaPtP consecutive prism slabs are directly superposed. Four other types of stacking, with 2, 3, 4 and 6 prism slabs respectively, in the translation unit, have been observed up to now. In hexagonal ZrBeSi [24], presented in Fig. 3, consecutive layers formed by the prism-centring atoms (beryllium and silicon) are rotated by 60° around the *c*-axis with respect to each other. This stacking sequence can be denoted as BC. In the deformation derivative NdPtSb [25] the corresponding layers are slightly puckered, whereas for its branch LiGaGe [26] the distortions are so strong that a three-dimensional framework of gallium and germanium atoms is observed. Each gallium and germanium atom is surrounded by a Ge_4 and Ga_4 tetrahedron respectively, and the structure can be considered as a ternary substitution variant of $CaIn_2$. The YLiSn structure, shown in Fig. 1 and discussed above, is another deformation variant of ZrBeSi, where a distorted tetrahedral framework is also observed.

For the orthorhombic TiNiSi type [27] and its branches, as can be seen from their [010] projections given in Fig. 4, the atoms forming the trigonal prisms are displaced from their ideal positions. The HoNiGa [28] branch can be obtained by a ternary substitution from the binary KHg_2 type which implies a lowering of the symmetry from a body-centred to a primitive orthorhombic lattice. The nickel atoms in TiNiSi are inside almost regular Si_4 tetrahedra and, in comparison with HoNiGa, shifted so that infinite zigzag chains with an interatomic distance of 2.67 Å are observed. Of the six large atoms forming the distorted trigonal prism around the silicon site, one is at a considerably longer distance and does not belong to the first coordination sphere. The coordination of this site is generally described as a trigonal Ti_4Ni_2 prism capped by one titanium and two nickel atoms, the prism axis of this mixed prism being perpendicular to the axis of the Ti_6 prism. In a similar way, the coordination around the titanium site should be considered a penta-capped pentagonal

prism of composition $Ti_4Ni_6Si_5$. The antitype BiSCl [29], a normal valence compound, is more closely related to the hexagonal Ni_2In type [30] and its orthorhombic distortion variant UPt_2 [31] where the majority atoms form the trigonal prisms corresponding to the aluminium atom prisms in AlB_2 and occupy half of the prism centres. The ternary isopointal substitution variant of UPt_2 is known as YAlGe [32].

A stacking with three trigonal prism slabs in the translation unit is found for trigonal CaLiSn [33] (see Fig. 4). Ignoring the displacements of the atoms away from the prism centres, similar to those observed in $CaIn_2$ and LiGaGe, the stacking sequence of the lithium and tin atom layers here is BCB. The lithium atoms and two thirds of the tin atoms are inside elongated tetrahedra of composition Sn_4 and Li_3Sn respectively, whereas the remaining tin atoms are surrounded by a trigonal Li_5 bipyramid. The four trigonal prism slabs in the translation unit of the hexagonal YPtAs type [25] are stacked in the sequence BBCC. The atom arrangement is close to that of AlB_2 and SrPtSb ($c/4a = 0.89$). The stacking in orthorhombic CaCuGe [34] corresponds to the sequence BBBCCC but, owing to the large distortions, the structure should rather be considered a substitution variant of KHg_2 and HoNiGa with a three times larger unit cell. No compound with undistorted slabs in the same stacking has yet been observed.

Another example of a substitution derivative of AlB_2 with non-equiatomic composition, $Tb_3Co_2Ge_4$ [35], is shown in Fig. 3. This monoclinic structure can be described as an intergrowth of TiNiSi- and AlB_2-type columns parallel to [010]: $2TbCoGe + TbGe_2 = Tb_3Co_2Ge_4$.

3.3. *Effect of substitution on the crystal structure*

Compounds crystallizing with one of the structure types discussed above contain 33.3 at.% of an element with a larger atomic radius. In the binary systems the compounds have the stoichiometry 1:2 and in the ternary systems they are to be found on the corresponding binary cross-section of the phase diagram. The majority of the rare-earth metal gallides and silicides RM_2 crystallize with structures of the AlB_2 family. Solid solutions are often observed when gallium or silicon is replaced by a small amount of a late transition metal (T). With a more extensive substitution, up to the composition RTM, new phases belonging to the same structure family may be obtained. Compounds with more than 33.3 at.% of transition metal generally adopt structures of the Laves-phase family, like the binary RT_2 compounds.

In each of the R–Co–Ga systems (R ≡ Y, Tb, Dy, Ho, Er, Tm, Yb, Lu) at least two compounds crystallizing with structure types of the AlB_2 family are found [2, 36, 37]. For example, in the Er–Co–Ga system studied at 873 K, four such compounds have been identified. Binary $ErGa_2$, with AlB_2-type structure ($c/a = 0.96$) [38], dissolves up to about 2 at.% cobalt. A second phase with an isopointal structure and a narrow homogeneity range is found at the composition $ErCo_{0.2}Ga_{1.8}$. For this compound the c/a ratio is considerably smaller (0.82) and corresponds to the UHg_2 type. Further substitution of gallium by cobalt leads to the formation of the Lu_2CoGa_3-type phase which has a homogeneity range from $ErCo_{0.3}Ga_{1.7}$ to $ErCo_{0.7}Ga_{1.3}$. Inside the homogeneity range the c/a ratio is constant (0.80), but the unit-cell volume decreases with higher cobalt content (see Table 3). The equiatomic ErCoGa crystallizes with a HoNiGa-type structure [39]. The same structure types are observed in the {Y, Tb, Dy, Ho}–Co–Ga systems. The Tm–Co–Ga system is similar to the preceding systems but no compound occurs at the equiatomic composition and the gallide $TmGa_2$ crystallizes with a KHg_2 type structure [40]. On the corresponding cross-section of the Yb–Co–Ga system at 673 K only two compounds have been found: $YbGa_2$ with $CaIn_2$-type structure [41] and the ternary phase with Lu_2CoGa_3-type structure.

In the same way as thulium, the binary gallide of lutetium forms a KHg_2-type structure [40]. The hexagonal structure of Lu_3CoGa_5 ($LuCo_{0.3}Ga_{1.7}$) [42], which is an ordered substitution variant of the Fe_2P type [43], can also be derived from an AlB_2-type atom arrangement by considering a ternary substitution and a subsequent displacement of the cobalt atoms into the rare-earth metal atom layers. A narrow two-phase region separates this compound from the homogeneity range of the Lu_2CoGa_3-type phase. At 873 K no compound is observed at the composition LuCoGa.

No systematic investigation of the Er–Rh–Si system has been carried out. A binary phase with AlB_2-type structure was only found for the off-stoichiometric composition $ErSi_{1.67}$ [44], whereas at high temperature $ErSi_2$ crystallizes with an α-$ThSi_2$-type structure [45], a stacking variant of AlB_2 with mutually perpendicular trigonal prism axes [46]. A HoNiGa-type structure was refined for the equiatomic compound ErRhSi [47]. No significant homogeneity range has been mentioned for Er_2RhSi_3. The c/a ratio for this compound is 0.96, *i.e.* 11% lower than for the binary, silicon-deficient AlB_2-type silicide (1.08).

In order to study the variation of the space-filling along the RT_2–RTM cross-section in the Er–Co–Ga and Er–Rh–Si systems, the average volume per trigonal prism V_{6p} was calculated for each compound and plotted *vs.* the cobalt (rhodium) content (see Fig. 5). The volume of the distorted prisms in ErCoGa is 13% lower than that of the straight prisms in $ErGa_2$. From comparison of the atomic radii of cobalt and gallium it

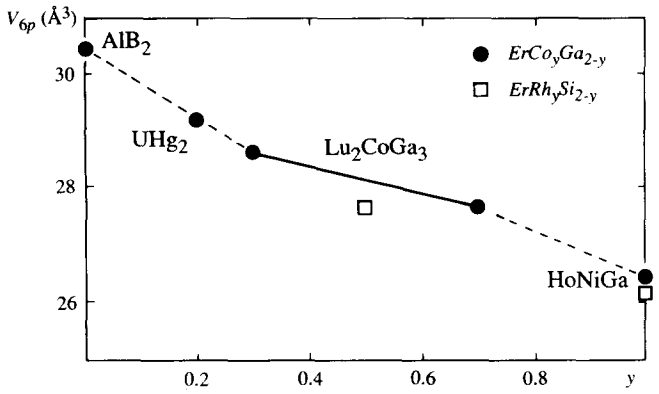

Fig. 5. The average trigonal prism volume V_{6p} calculated for $ErCo_yGa_{2-y}$ compounds, plotted as a function of the cobalt content ($0 \leqslant y \leqslant 1$). The solid line corresponds to the homogeneity range of the Lu_2CoGa_3-type phase. Squares indicate the values calculated for Er_2RhSi_3 and ErRhSi.

can be estimated that a simple substitution of half of the gallium atoms by cobalt atoms inside straight prisms would lead to a smaller reduction in prism volume. The better space-filling is obtained by the step by step deformation of the ideal trigonal prisms. In the UHg_2-type structure $ErCo_{0.2}Ga_{1.8}$, the trigonal prisms are compressed along the prism axis with contact distances Er–Er in this direction (3.58 Å). In the $Er_2Co_{0.6-1.4}Ga_{3.4-2.6}$ phase three-quarters of the erbium atoms are displaced from their ideal positions and now have their contact distances in the (0001) plane (3.52 Å for $Er_2Co_{1.4}Ga_{2.6}$). For the remaining quarter of the erbium atoms the shortest distances are still observed along [0001] (3.45 Å). All erbium atoms are displaced in the ErCoGa structure and have short interatomic distances inside the distorted triangle mesh layers (3.36 Å) and between these layers (3.61 Å). A similar decrease in the average trigonal prism volume is observed between Er_2RhSi_3 with slightly distorted prisms and ErRhSi with strongly distorted prisms, even if in this case the atomic radius of the transition metal is slightly larger than that of the non-metal element.

It might be of interest to note that also for equiatomic CrB- and FeB-type compounds the volume of the trigonal rare-earth metal atom prisms decreases while main-group elements are replaced by transition metals at the prism centres [48].

Acknowledgments

We thank Dr. H. D. Flack for useful discussions and acknowledge the help of Ms. Birgitta Künzler with the preparation of the drawings. The experimental work on gallides was carried out at L'vov University (Ukraine). The studies done at Geneva University were supported by the Swiss National Science Foundation under contract 20-28490.90 and the Alfred and Hilde Freissler Stiftung.

References

1 B. Chevalier, P. Lejay, J. Etourneau and P. Hagenmuller, *Solid State Commun., 49* (1984) 753–760.
2 R. E. Gladyshevskii, *Thesis*, Moscow State University, Moscow, 1987.
3 R. E. Gladyshevskii and B. I. Chernyak, *XI Ukrainian Republic Conf. on Inorganic Chemistry, Kiev, 1986, Collected Abstracts*, p. 49.
4 E. Blanc, D. Schwarzenbach and H. D. Flack, *J. Appl. Crystallogr., 24* (1991) 1035–1041.
5 J. A. Ibers and W. C. Hamilton (eds.), *International Tables for X-ray Crystallography*, Vol. IV, Kynoch, Birmingham, 1974 (present distributor Reidel, Dordrecht).
6 Th. Hahn (ed.), *International Tables for Crystallography*, Vol. A, Reidel, Dordrecht, 1983 (present distributor Kluwer, Dordrecht).
7 S. R. Hall and J. M. Stewart (eds.), *XTAL3.0 User's Manual*, Universities of Western Australia and Maryland, 1990.
8 L. M. Gelato and E. Parthé, *J. Appl. Crystallogr., 20* (1987) 139–143.
9 V. K. Pecharskii, P. Yu. Zavalii, L. G. Aksel'rud, Yu. N. Grin' and E. I. Gladyshevskii, *Vestn. L'vov. Univ., Ser. Khim., 25* (1984) 9–11.
10 G. Steinberg and H. U. Schuster, *Z. Naturforsch., B34* (1979) 1165–1166.
11 M. L. Fornasini and F. Merlo, *Acta Crystallogr., B36* (1980) 1739–1744.
12 F. E. Wang, F. A. Kanda, C. F. Miskell and A. J. King, *Acta Crystallogr., 18* (1965) 24–31.
13 E. J. Duwell and N. C. Baenziger, *Acta Crystallogr., 8* (1955) 705–710.
14 P. I. Kripyakevich, *Structure Types of Intermetallic Compounds*, Nauka, Moscow, 1977.
15 E. Hovestreydt, N. Engel, K. Klepp, B. Chabot and E. Parthé, *J. Less-Common Met., 85* (1982) 247–274.
16 W. Hofmann and W. Jäniche, *Naturwissenschaften, 23* (1935) 851.
17 R. E. Rundle and A. S. Wilson, *Acta Crystallogr., 2* (1949) 148–150.
18 A. Iandelli and R. Ferro, *Gazz. Chim. Ital., 84* (1954) 463–478.
19 E. I. Gladyshevskii, *Dopov. Akad. Nauk Ukr. RSR, 2* (1964) 209–212.
20 A. Iandelli, *Z. Anorg. Allg. Chem., 330* (1964) 221–232.
21 T. I. Yanson, *Thesis*, L'vov State University, L'vov, 1975.
22 G. Wenski and A. Mewis, *Z. Anorg. Allg. Chem., 535* (1986) 110–122.
23 G. Wenski and A. Mewis, *Z. Anorg. Allg. Chem., 543* (1986) 49–62.
24 J. W. Nielsen and N. C. Baenziger, *U.S.A.E.C.*, (1953) 2728–2732.
25 G. Wenski and A. Mewis, *Z. Kristallogr., 176* (1986) 125–134.
26 W. Bockelmann, H. Jacobs and H. U. Schuster, *Z. Naturforsch., B25* (1970) 1305–1306.
27 C. Brink Shoemaker and D. P. Shoemaker, *Acta Crystallogr., 18* (1965) 900–905.
28 Ya. P. Yarmolyuk, Yu. N. Grin' and E. I. Gladyshevskii, *Dopov. Akad. Nauk Ukr. RSR, Ser. A, 9* (1979) 771–775.
29 E. Dönges, *Z. Anorg. Chem., 263* (1950) 112–132.
30 E. S. Makarov, *Izv. Akad. Nauk SSSR, Ser. A, 1* (1944) 29–33.

31 B. A. Hatt and G. I. Williams, *Acta Crystallogr., 12* (1959) 655–657.
32 J. T. Zhao and E. Parthé, *Acta Crystallogr., C46* (1990) 2276–2279.
33 W. Müller and R. Voltz, *Z. Naturforsch., B29* (1974) 163–165.
34 W. Dörrscheidt, N. Niess and H. Schäfer, *Z. Naturforsch., B32* (1977) 985–988.
35 P. K. Starodub, I. R. Mokraya, O. I. Bodak, V. K. Pecharskii and V. A. Bruskov, *Sov. Phys. Crystallogr., 31* (1986) 231–232.
36 Yu. N. Grin' and R. E. Gladyshevskii, *Gallides,* Metallurgia, Moscow, 1989.
37 R. E. Gladyshevskii, Yu. N. Grin' and Ya. P. Yarmolyuk, *Stable and Metastable Phase Equilibrium in Metallic Systems,* Nauka, Moscow, 1985, pp. 49–54.
38 S. E. Haszko, *Trans. Metall. Soc. AIME, 221* (1961) 201–202.
39 O. M. Sichevich, R. E. Gladyshevskii, Yu. N. Grin' and Ya. P. Yarmolyuk, *Dopov. Akad. Nauk Ukr. RSR, Ser. B, 11* (1982) 60–62.
40 E. I. Gladyshevskii, Yu. N. Grin', S. P. Yatsenko, Ya. P. Yarmolyuk and K. A. Chuntonov, *Dopov. Akad. Nauk Ukr. RSR, Ser. A, 6* (1980) 82–85.
41 A. Iandelli, *Z. Anorg. Allg. Chem., 330* (1964) 221–232.
42 R. E. Gladyshevskii, *IV All-Union Conf. on Crystal Chemistry of Intermetallic Compounds, L'vov, October 18–20, 1983, Collected Abstracts,* pp. 48–49.
43 S. Rundqvist and F. Jellinek, *Acta Chem. Scand., 13* (1959) 425–432.
44 E. I. Gladyshevskii, *Dopov. Akad. Nauk Ukr. RSR, 7* (1963) 886–888.
45 R. Nesper, H. G. von Schnering and J. Curda, *VI Int. Conf. on Solid Compounds of Transition Elements, Stuttgart, June 12–16, 1979,* pp. 150–152.
46 G. Brauer and A. Mitius, *Z. Anorg. Chem., 249* (1942) 325–339.
47 W. Bazela, J. Leciejewicz and A. Szytula, *Acta Phys. Pol., A68* (1985) 575–581.
48 E. Parthé, in M. O'Keeffe and A. Navrotsky (eds.), *Structure and Bonding in Crystals,* Vol. II, Academic Press, New York, 1981, Chapter 25, pp. 256–296.